Electronic Supplementary Material (ESI) for Journal of Materials Chemistry A.

3D low toxicity Cu-Pb binary perovskite films and their photoluminescent/photovoltaic performance

Xin Ge[1,2], Xin Qu[1,2], Li He[1,2], Yansen Sun [1,2], Xin Guan[1,2], Zhenyu Pang[1,2],Ce Wang[1,2], Lili Yang[1,2],*

*Fengyou Wang[1,2]*and Federico Rosei[1,3]**

[1]Key Laboratory of Functional Materials Physics and Chemistry of the Ministry of Education, Jilin Normal University, Changchun 130013, China

[2]National Demonstration Center for Experimental Physics Education, Jilin Normal University, Siping 136000, PR China

[3]Centre Énergie, Materiaux et Télécommunications, Institut National de la Recherche Scientifique, 1650, Boulevard Lionel-Boulet, Varennes, Québec J3X 1S2, Canada

*To whom correspondence should be addressed.

E-mail: llyang1980@126.com (L.L. Yang); wfy@jlnu.edu.cn (F. Y. Wang); rosei@emt.inrs.ca (F.R.)

Supporting information

Preparation of perovskite solar cells

The 2×2 cm^2 FTO substrates were firstly cleaned with ultrasonic technique in deionized water, detergent, acetone and alcohol for 20 minutes, then were treated with ozone for 20 minutes.

Preparation of the electron transport layer: the SnO_2 aqueous solution was mixed with deionized water in a ratio of 1:1, which was spin-coated on the clean FTO substrates at a low speed of 500 rpm for 3 s firstly, and then at a high speed of 5000 rpm for 30 s. Annealing process was carried out at 150 ° for 30 minutes on a heating stage.

Preparation of the perovskite layer: The perovskite precursor solution was dissolved in a mixed solvent of DMSO and DMF (9:1 v: v) by of MAI (0.163 g), PbI_2 and $CuCl_2$. The doping ratio of $CuCl_2$ to PbI_2 was 0%, 5%, 10%, 15%, and 20%, respectively. The spin-coating speed was initially increased to 500 rpm for 3 s, then increased to 3000 rpm for 30 s. The anti-solvent chlorobenzene was added in the 24th s.

Preparation of hole transport layer: spiro (0.723 g) was mixed with 1 ml chlorobenzene solvent, tetra-tert-butyl pyridine(28.5 μl) and Li salt solution (19.5 μl). The Li salt solution was prepared by mixing Li salt (0.52 g) with 1 ml of acetonitrile. Spin coating was performed at the same rotational speed as the one used for the electron transport layer. Finally, an Ag electrode was deposited by vapor deposition.

Theoretical calculations

Density functional theory calculations were performed using the Vienna ab initio simulation package, to optimize structure and proceed energy calculations.[1] The ion-electron interaction was described with the projector-augmented plane wave (PAW).[2]

Characterization and Testing

The surface morphology and elemental composition of the samples were investigated by FESEM (Hitachi s-570) and EDS. The crystal structure was examined

by X-ray diffraction (Rigaku D / MAX 3C X-ray diffractometer with Cu K_α radiation). UV-Vis absorption spectroscopy was measured using a UV-5800 pc spectrophotometer. A spectrometer (Horiba Jobin Yvon Fluorolog-3) with a time-correlated single-photon counting lifetime spectroscopy system was used to collected PL and TRPL spectra. The chemical composition of all thin films was characterized by X-ray photoelectron spectrometer (XPS) (Esca lab 250 XI) using Mg K_α radiation (1253.6 eV) with a resolution of 1.0 eV. The photocurrent density vs. voltage curve was measured by AM 1.5G simulated illumination (100 mW /cm^2, Model 91160, Newport). An external quantum efficiency (EQE) measurement was performed on QEX10 system.

The corresponding SEM images of all films were shown in Figure S1. As shown in Fig. S1, the perovskite film presented Leaf-like morphology with the volume ratio of DMF:DMSO of 5:5. With increasing the volume ratio of DMF:DMSO to 10:0, the perovskite film showed the morphology composing of closely packed dendritic grain, indicating that the morphology of the $MAPb_{0.9}Cu_{0.1}I_{3-2x}Cl_{2x}$ perovskite film can be controlled by DMF/DMSO ratio.

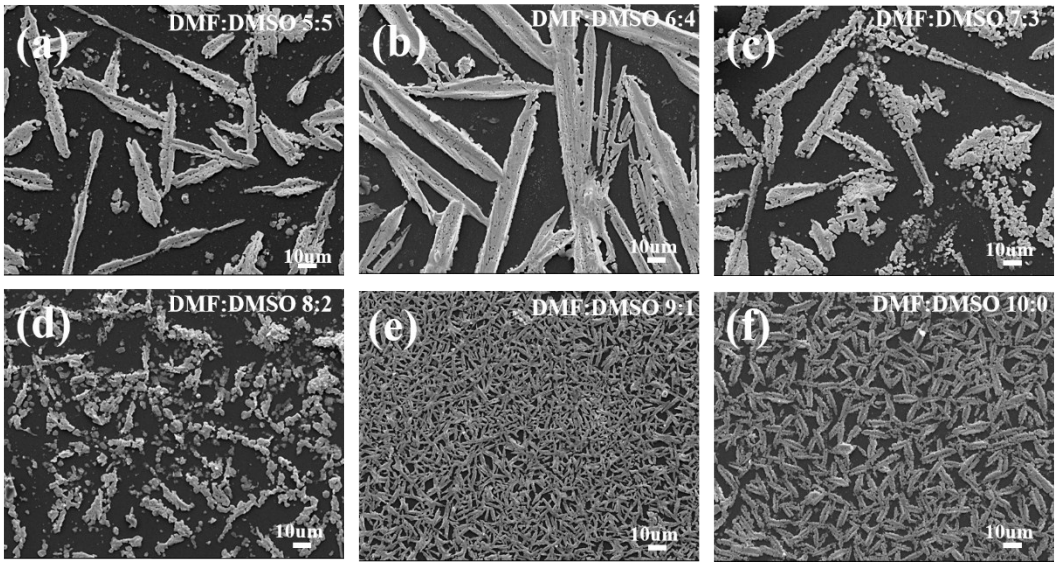

Figure S1. SEM images of $MAPb_{0.9}Cu_{0.1}I_{3-2x}Cl_{2x}$ perovskite film prepared with using different DMF/DMSO ratio (a-f) without chlorobenzene (CB) anti-solvent treatment.

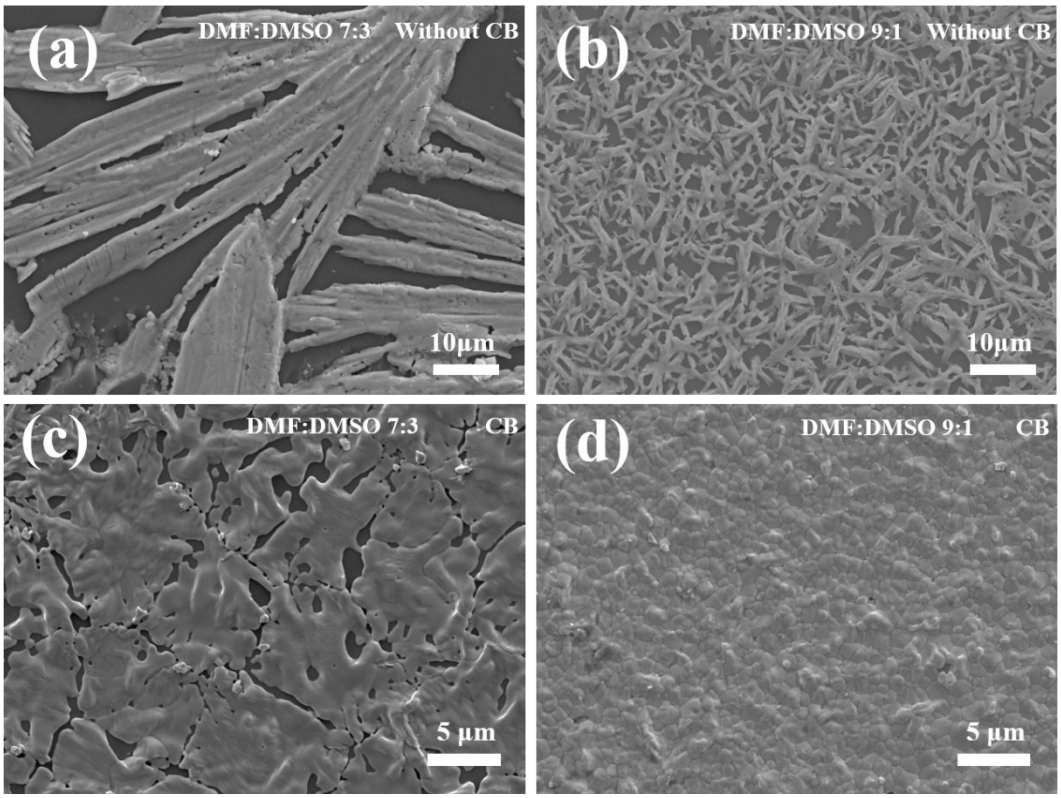

Figure S2. SEM images of $MAPb_{0.9}Cu_{0.1}I_{3-2x}Cl_{2x}$ perovskite film prepared with using different DMF/DMSO ratio with or without chlorobenzene (CB) anti-solvent treatment. (a) 7:3 (b) 9:1 (c) 7:3/CB (d) 9:1/CB.

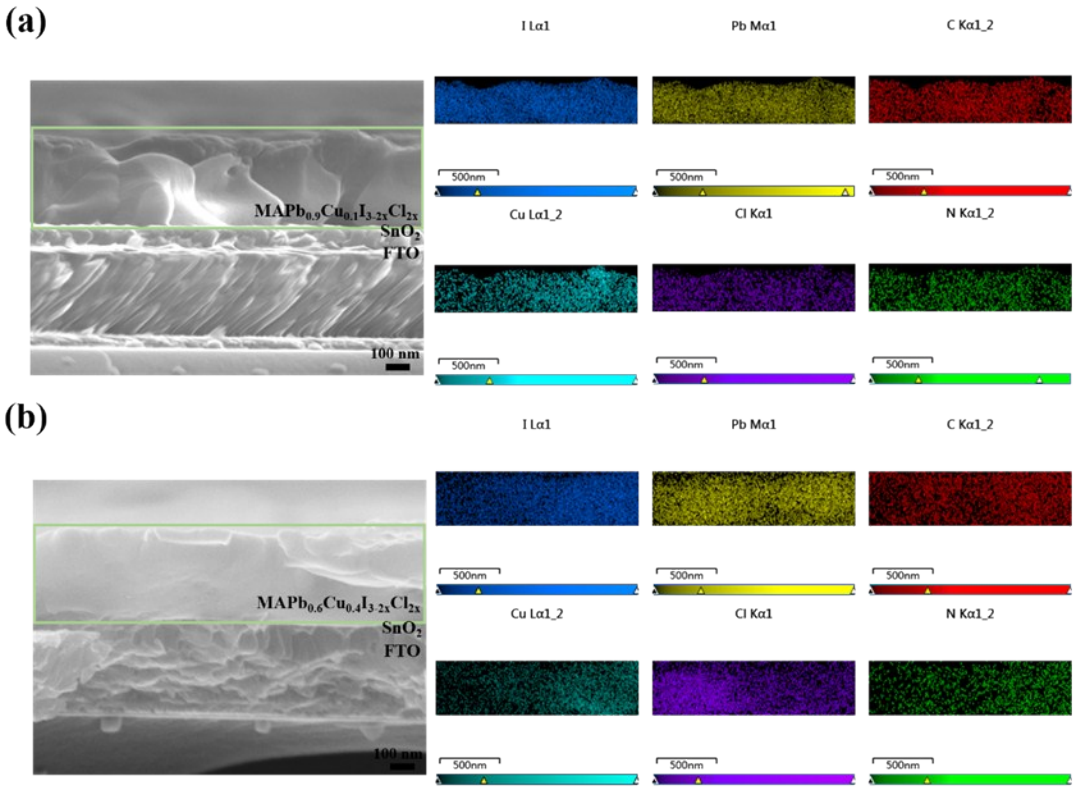

Figure S3. The image of cross-sectional Scanning Electron Microscope (SEM) and Energy Dispersion Spectrum (EDS) of Cu doping perovskite material. (a) $MAPb_{0.9}Cu_{0.1}I_{3-2x}Cl_{2x}$, (b) $MAPb_{0.6}Cu_{0.4}I_{3-2x}Cl_{2x}$.

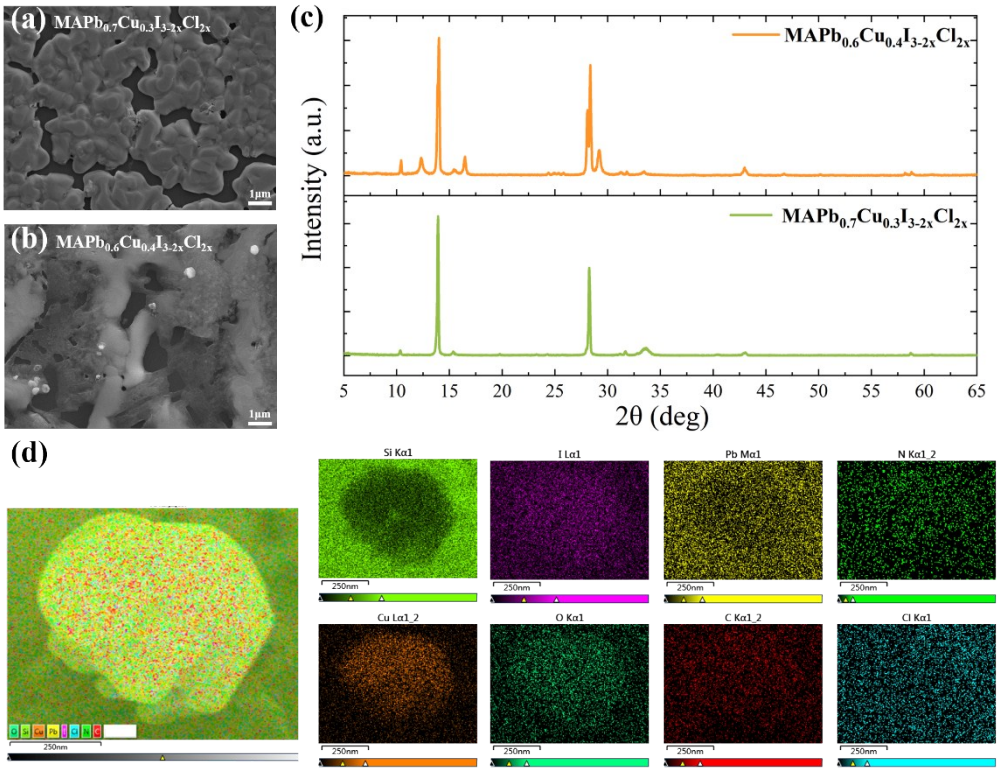

Figure S4. (a) SEM image of $MAPb_{0.7}Cu_{0.3}I_{3-2x}Cl_{2x}$, (b) SEM image of $MAPb_{0.6}Cu_{0.4}I_{3-2x}Cl_{2x}$, (c)XRD patterns of $MAPb_{0.7}Cu_{0.3}I_{3-2x}Cl_{2x}$ and $MAPb_{0.6}Cu_{0.4}I_{3-2x}Cl_{2x}$. (d) The Energy Dispersion Spectrum (EDS) of the white particle in $MAPb_{0.6}Cu_{0.4}I_{3-2x}Cl_{2x}$.

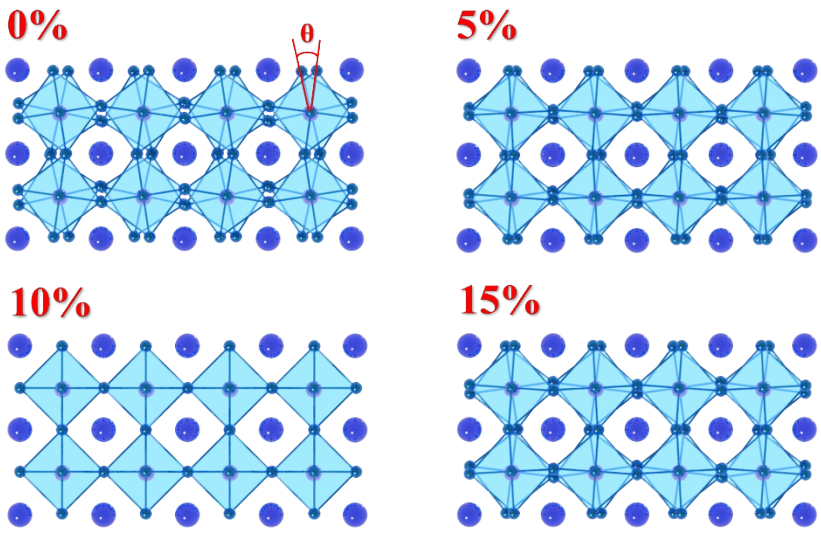

Figure S5. Top view of the mechanism of copper-chlorine co-doping concentration on the symmetry of perovskite crystal structure

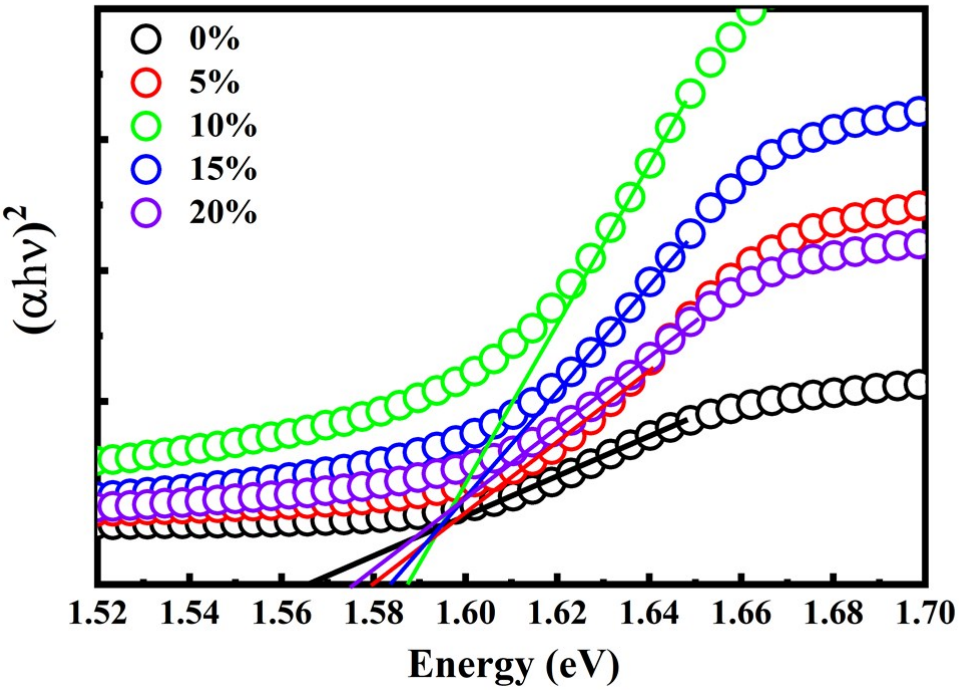

Figure S6. Tauc plot curves of $MAPb_{1-x}Cu_xI_{3-2x}Cl_{2x}$.

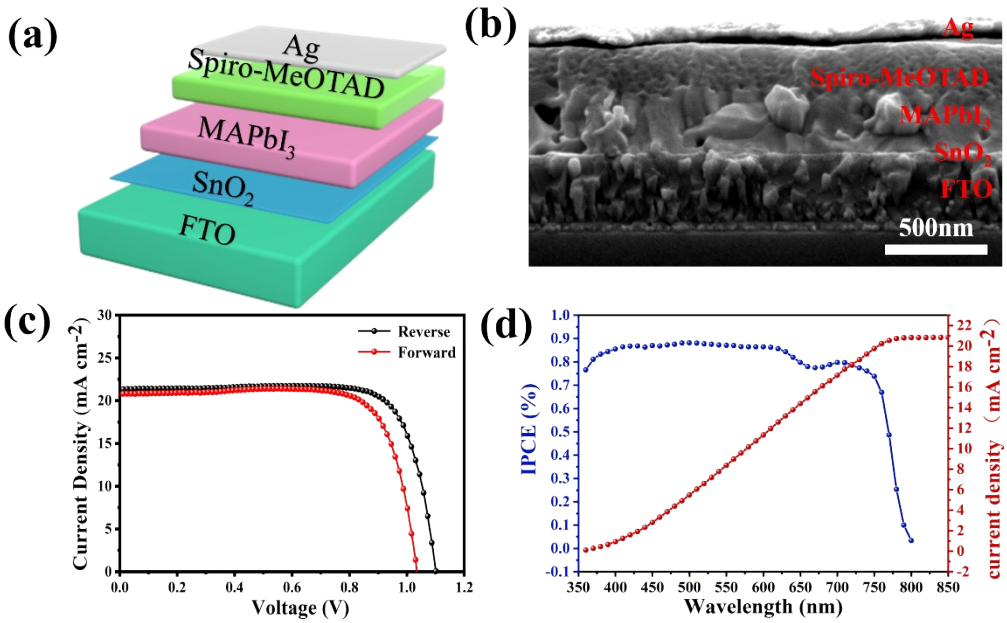

Figure S7. (a) Schematic diagram of $MAPbI_3$ perovskite solar cells structure (b) SEM sectional view of $MAPbI_3$ perovskite solar cells (c) Current-voltage curve of $MAPbI_3$ perovskite solar cells. (d) The EQE plot of the $MAPbI_3$ perovskite solar cell.

Table S1. Photovoltaic parameters obtained from $MAPbI_3$

Perovskite type		V_{oc} (V)	J_{sc} (mA cm^{-2})	FF (%)	PCE (%)
$MAPbI_3$	Reverse scan	1.09	21.42	78.53	18.49
	Forward scan	1.03	20.92	77.69	16.78

Table S2. Specific parameters of Hall Effect measurements

Samples	Carrier concentration(cm^{-3})	Mobility($cm^{-2}V^{-1}s^{-1}$)	Type
$MAPbI_3$	2.46×10^{15}	1.42×10^{2}	n
$MAPb_{0.95}Cu_{0.05}I_{3-2x}Cl_{2x}$	9.33×10^{14}	2.55×10^{2}	n
$MAPb_{0.9}Cu_{0.1}I_{3-2x}Cl_{2x}$	9.49×10^{13}	4.06×10^{2}	n
$MAPb_{0.85}Cu_{0.15}I_{3-2x}Cl_{2x}$	3.00×10^{13}	2.66×10^{2}	n
$MAPb_{0.75}Cu_{0.25}I_{3-2x}Cl_{2x}$	1.25×10^{13}	1.72×10^{2}	n

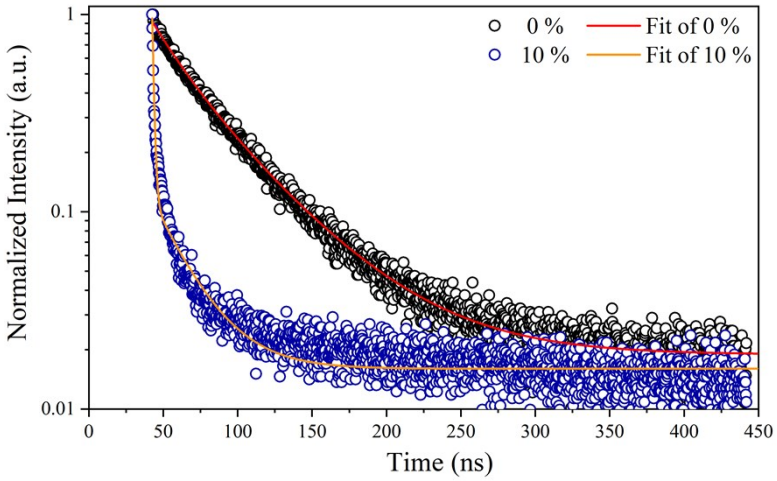

Figure S8. Time-resolved PL spectra of $MAPb_{1-x}Cu_xI_{3-2x}Cl_{2x}$ (x=0, 0.10) on the SnO_2 electron transport layer. The corresponding double exponential fitting lines are presented as well.

Table S3. Fitting parameters of time-resolved PL spectra of $MAPb_{1-x}Cu_xI_{3-2x}Cl_{2x}$ (x=0, 0.10) on the SnO_2 electron transport layer

	A_1	τ_1(ns)	A_2	τ_2(ns)	τ_{ave} (ns)
$MAPbI_3$	35%	20.7	65%	51.3	45.8
$MAPb_{0.9}Cu_{0.1}I_{3-2x}Cl_{2x}$	90%	1.1	10%	24.5	17.8

References

1. G. Kresse and J. Furthmüller, *Phys. Rev. B*, 1996, **54** 11169-11186.
2. G. Kresse and D. Joubert, *Phys. Rev. B*. 1999, **59** 1758-1775.